Real-Time Monitoring of Protein–Liposome Interaction Kinetics Using Absorption, Polarized Intrinsic Emission, and Scattering (APIES): *Insights into Protein Corona Formation.*

Huajie F. Wang and Alan G. Ryder*.

Nanoscale Biophotonics Laboratory, University of Galway, University Road, Galway, H91 TK33, Ireland.

Tel: 353-(0)91-492943

Email: alan.ryder@universityofgalway.ie

April 2026 Version.

SUPPORTING INFORMATION.

(version for review/publication)

1.1 Estimation of lipids per liposome & HSA per monolayer.

We assume that HSA has a heart like shape 3.8 × 15 nm in size.[1-3] The number of lipids per liposome (N_{tot}) was estimated according to the method of Mozaffari et al.,[4] which was also used in our previous study.[5] In this model, N_{tot} is derived from the liposome surface area and the average phospholipid headgroup area, incorporating bilayer thickness to approximate the liposome geometry (**Equation S1**). The expression was further simplified to yield **Equation S2**, which was used for our calculations:

$$N_{Tot} = \left[\left(4\pi\left(\frac{d}{2}\right)^2\right) + \left(4\pi\left(\left(\frac{d}{2}\right) - h\right)^2\right)\right]/a \qquad \textbf{Equation S1}$$

$$N_{Tot} = 17.69 \times \left[\left(\frac{d}{2}\right)^2 + \left(\frac{d}{2} - 5\right)^2\right] \qquad \textbf{Equation S2}$$

Table S1: Surface areas of liposome and HSA binding surface using calculations made from the HSA circular area (πr^2), end-on binding (πa^2), and side-on binding (πab), all calculated using the Z_{av} diameter. The calculated amount of HSA required for a uniform monolayer on the liposome surface is given for each case. (a=1.9 nm, b=7.5 nm).

Surface area liposome (nm^2)	**Surface area HSA (nm^2)**			**Max. HSA per monolayer**		
	Circ. (πr^2)	**End-on** (πa^2)	**Side-on** (πab)	**Circ.** (πr^2)	**End-on** (πa^2)	**Side-on** (πab)
I = 25 mM						
70555	83.3	11.3	44.8	847	6224	1577
HSA: Liposome ratio: 7078:1 →8103:1						
I = 50 mM						
76807	84.9	11.3	44.8	905	6776	1717
HSA: Liposome ratio: 7241:1 →9381:1						
I = 100 mM						
68965	84.9	11.3	44.8	812	6084	1541
HSA: Liposome ratio: 6563:1 → 8298:1						
I = 150 mM						
83324	*80.1*	11.3	44.8	*1040*	*7350*	*1862*
HSA: Liposome ratio: 8408:1 → 9615:1						

1.2 DLS analysis of liposomes and HSA size distribution (distribution fits).

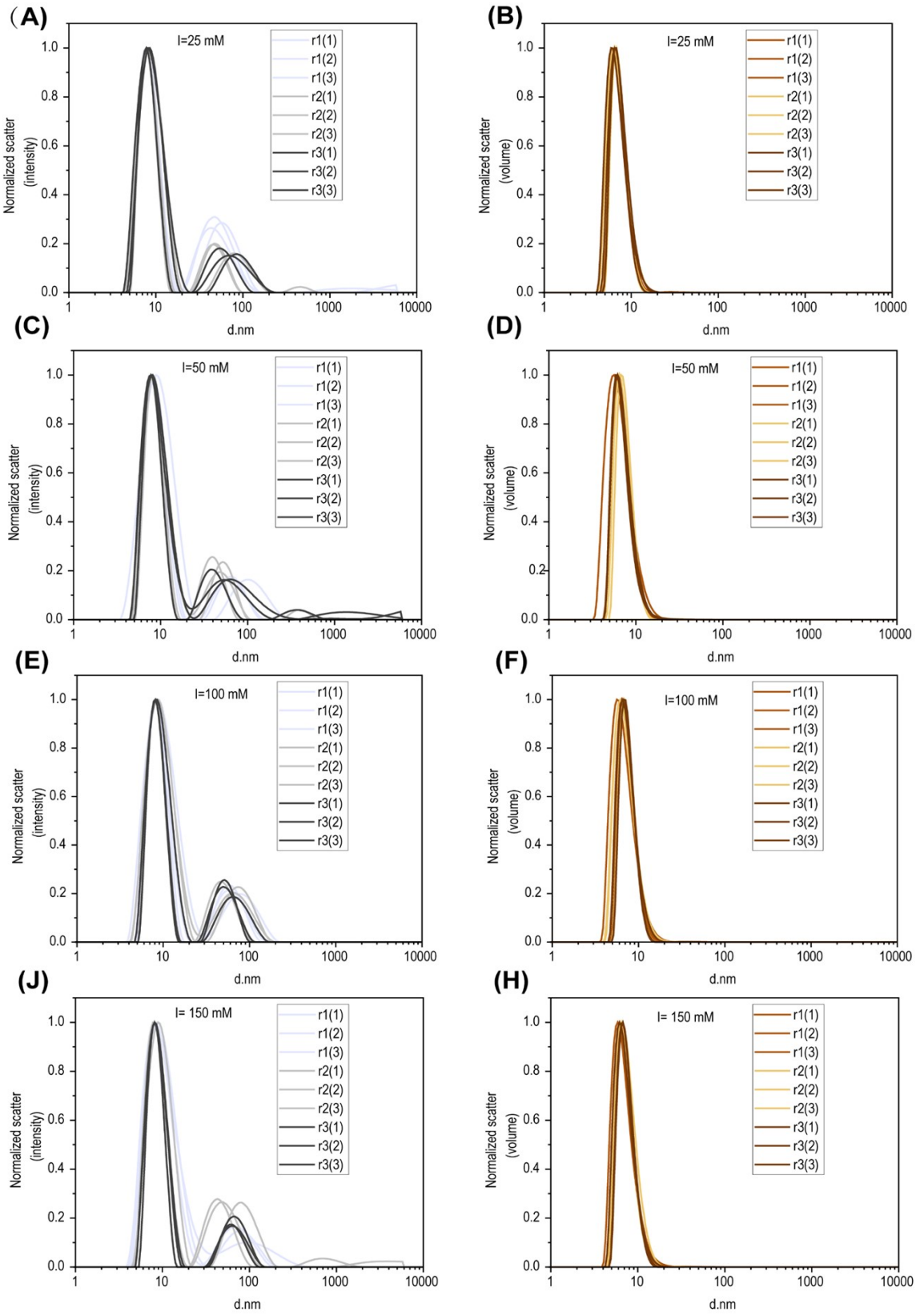

Figure S-1: Intensity-based (left) and volume-based (right) particle size distributions from DLS measurements of the HSA stock solutions. Data is from three separate stock solutions of HSA; each measured in triplicate.

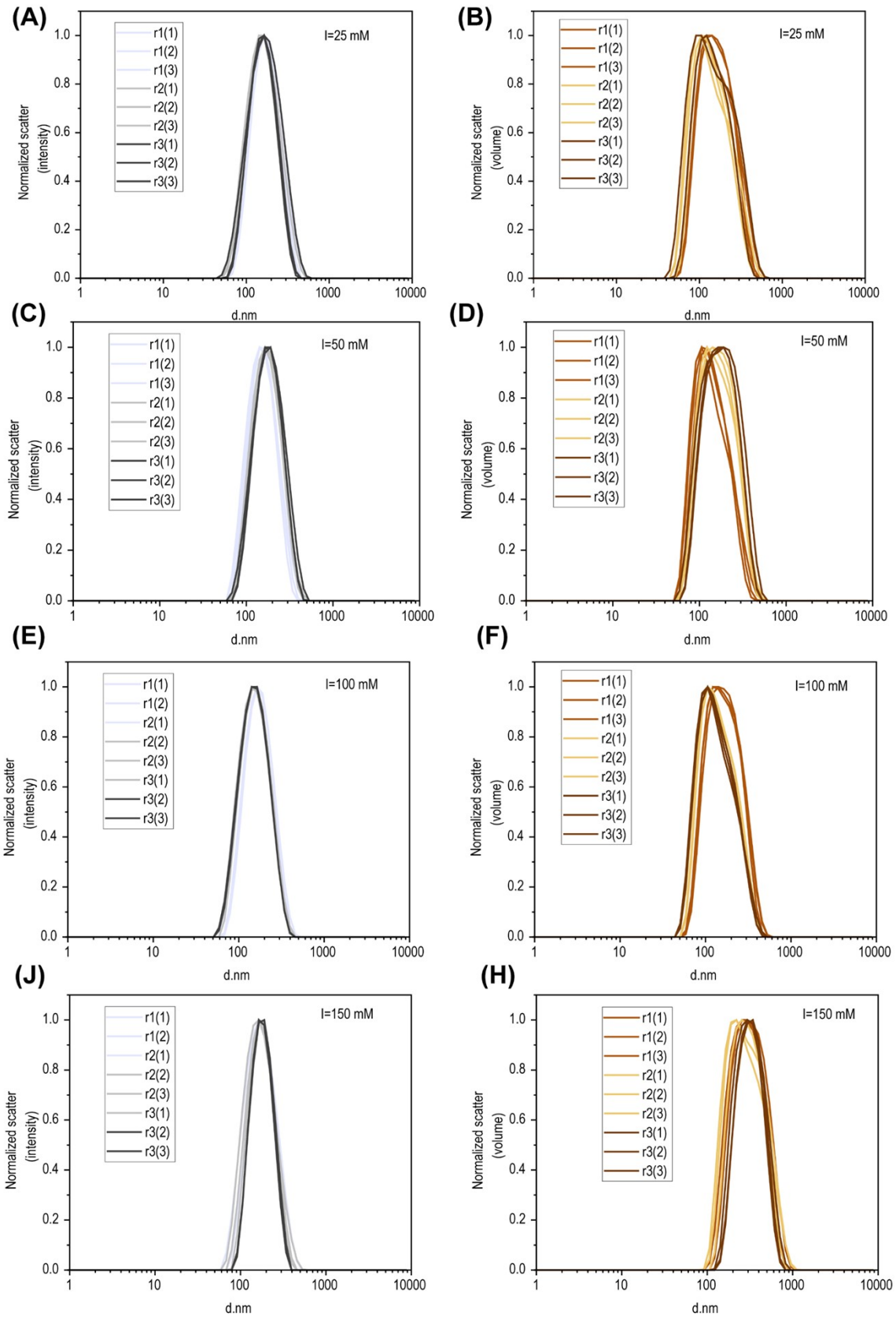

Figure S-2: Intensity-based (left) and volume-based (right) particle size distributions from DLS measurements of the pure liposomes in the four different buffers. Data is from three separate liposome preparations; each measured in triplicate.

1.3 Bimodal particle size resolution:

According to the following equation for a bi-modal distribution, the intensity of a component [45]:

$$\%Ia = \frac{Na \times a^6}{Na \times a^6 + Nb \times b^6} \times 100$$

where a and b represent the hydrodynamic radii of components and N_a and N_b the respective particle numbers. The intensity contribution of each component is strongly size-dependent, scaling with the sixth power of the hydrodynamic radius.[6] However, its ability to resolve bimodal or multicomponent mixtures is fundamentally limited by the physics of light scattering. Normally DLS reports an **intensity-weighted** distribution in which the scattered intensity scales approximately with the sixth power of particle diameter under Rayleigh conditions $(I \propto d^6)$. Therefore, even a very small population of large particles will dominate the signal, obscuring the presence of smaller species. This intrinsic weighting greatly limits the resolving power of DLS. In our system, there is a large size difference between HSA (**~10 nm**) and liposomes (**~150 nm**) which yields an intensity ratio of ~10^7. Despite the excess HSA present (**Table S1**), after mixing, generally only a single band (*i.e.* liposome) was obtained from the liposomes-HSA mixtures. Furthermore, because of this intrinsically low resolution, and the size ranges involved here, DLS could not unambiguously distinguish between particles of similar sizes, such as between bare, partly coated, or fully protein coated liposomes.

1.4 Spectral changes in the first 200 seconds after mixing:

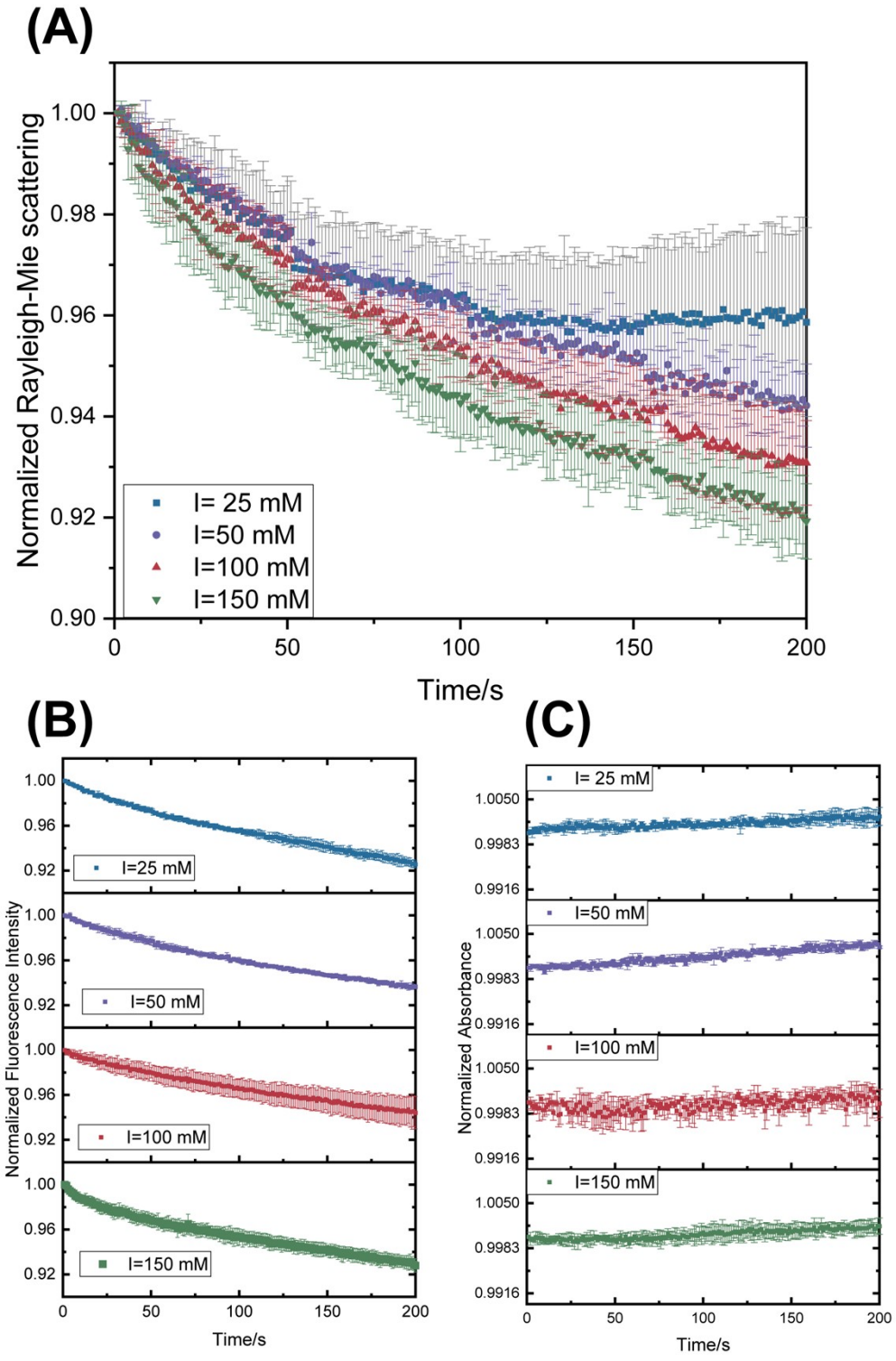

Figure S-3: (A) Normalized (to t_0) Rayleigh-Mie band intensity versus time from PIE_{VV} measurements immediately after mixing for the four buffer conditions; （B）Normalized Fluorescence versus time from PIE_{VV} measurements; (C) Normalized absorbance versus time from PIE_{VV} measurements.

1.5 Derived Count Rate and particle size changes.

The derived count rate (DCR) from DLS measurements is a useful parameter to compare the signal strength from different samples: the higher derived count rate usually indicates higher concentration, larger particles, or higher concentration and larger particles. From **Figure S4A**, DCR decreased about 30 % across all the buffer solutions. The idealized Rayleigh-scattering condition which assumes particles much smaller than the light wavelength, and that changes occur only in particle radius (R) while the particle number (N) while the refractive index contrast remains constant, leads to an expression for scattered light intensity (I):

$$I \propto NR^6$$

$$\frac{I_2}{I_1} = (\frac{R_2}{R_1})^6$$

Using the normalized DCR data ($^{I_2}/_{I_1} \approx 0.7$), the corresponding radius change would be:

$$\frac{R_2}{R_1} \approx 0.7^{1/6} \approx 0.94$$

Thus, even a ~30% decrease in scattering intensity would correspond to only an approximately 6% decrease in particle radius under these highly restrictive assumptions. **Figure S4**B, shows that the Zav (D_h) decreased by about 10 % during the first 200 seconds, which is of the same order of magnitude as the Rayleigh-based estimate.

These approximations should not be over-interpreted quantitatively, since the liposomes (D_h >100 nm) are more Mie like scatterers and thus other factors such as refractive-index contrast, polydispersity, and the presence of transient aggregates play a significant role.

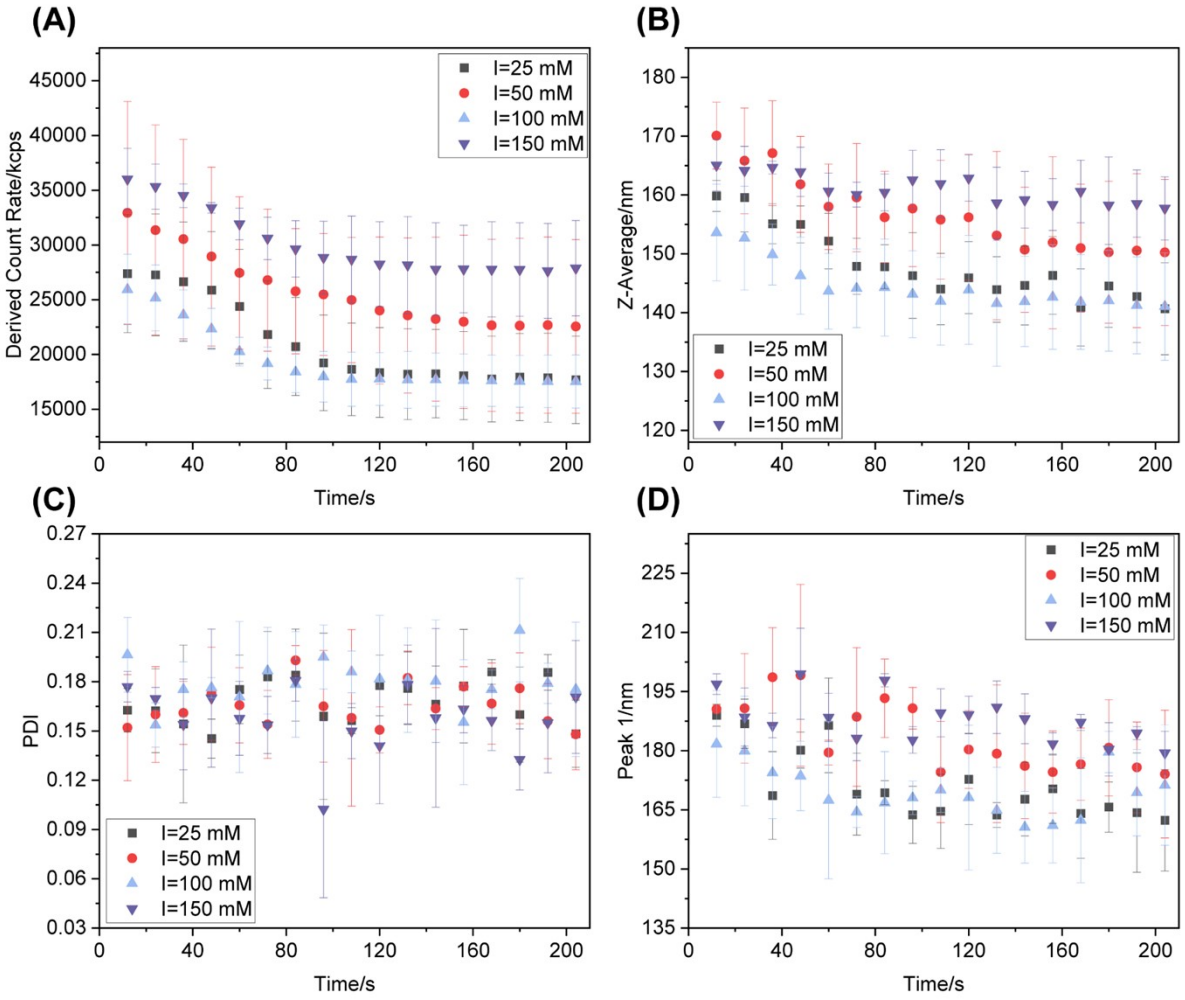

Figure S-4*:* DLS monitoring of protein–liposome interactions during the first 100 seconds after mixing under different buffer conditions. (A) Derived count rate; (B) polydispersity index (PDI); (C) average D_h (Zav.) from cumulants fit; and (D) Peak 1 from the distribution (intensity) fit. Each marker represents a single 10 s acquisition.

1.6 Size changes in the first 30 minutes after mixing:

DLS data were collected every 10 seconds after mixing for 30 minutes. This resulted in less accurate values for size and PdI, but it was sufficiently reliable to show gross size trends and the differences between the different ionic strength conditions.

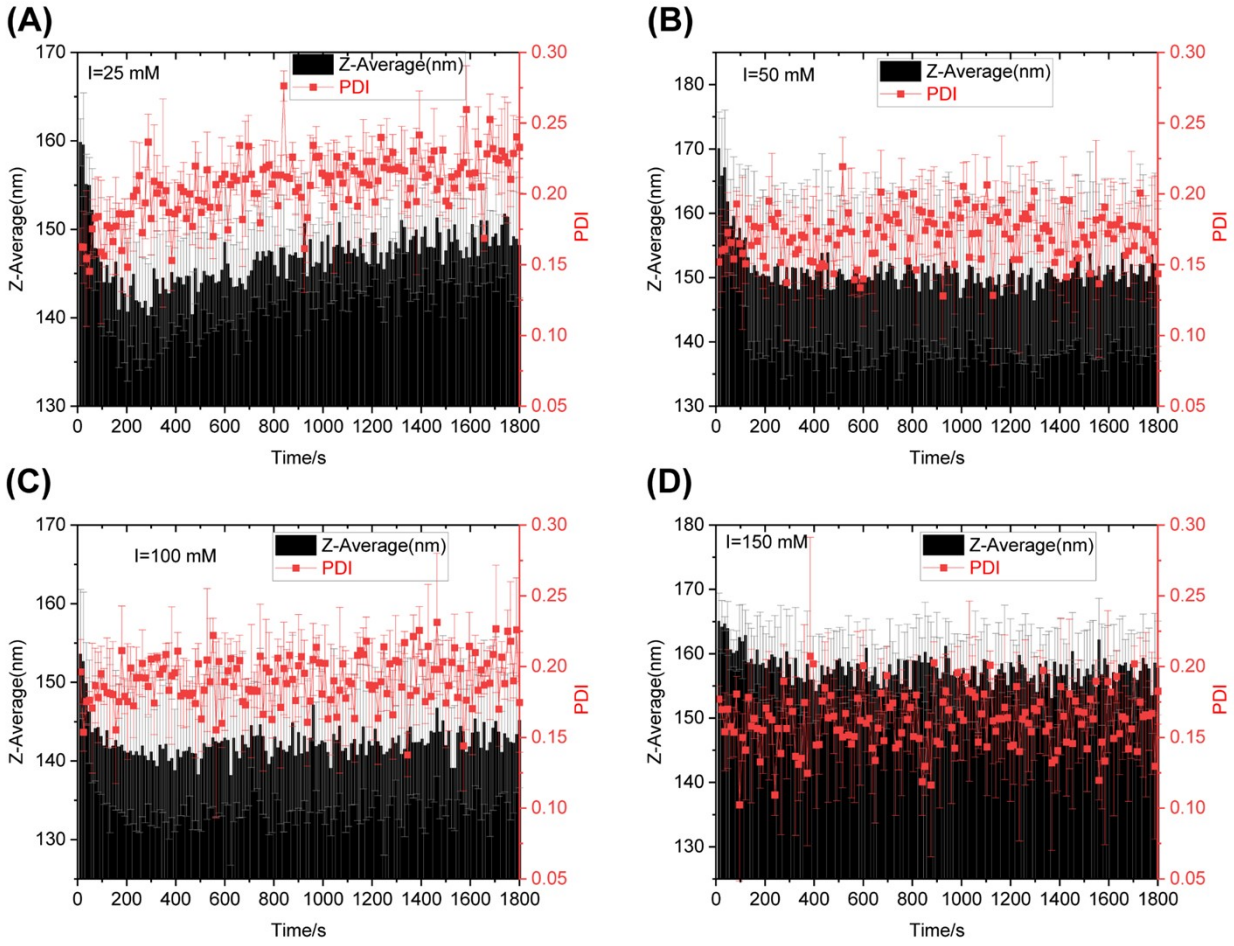

Figure S-5: Liposome size and polydispersity changes versus time for the 0-1800 s. period after mixing, for all four buffer conditions. Each datapoint is a single 10 s. DLS data collection, black bars are the $Z_{av.}$ (nm) and the red squares shown the polydispersity index (PdI).

1.7 Spectral changes in the 0-30 minutes, and 0.5 to 3 hour periods:

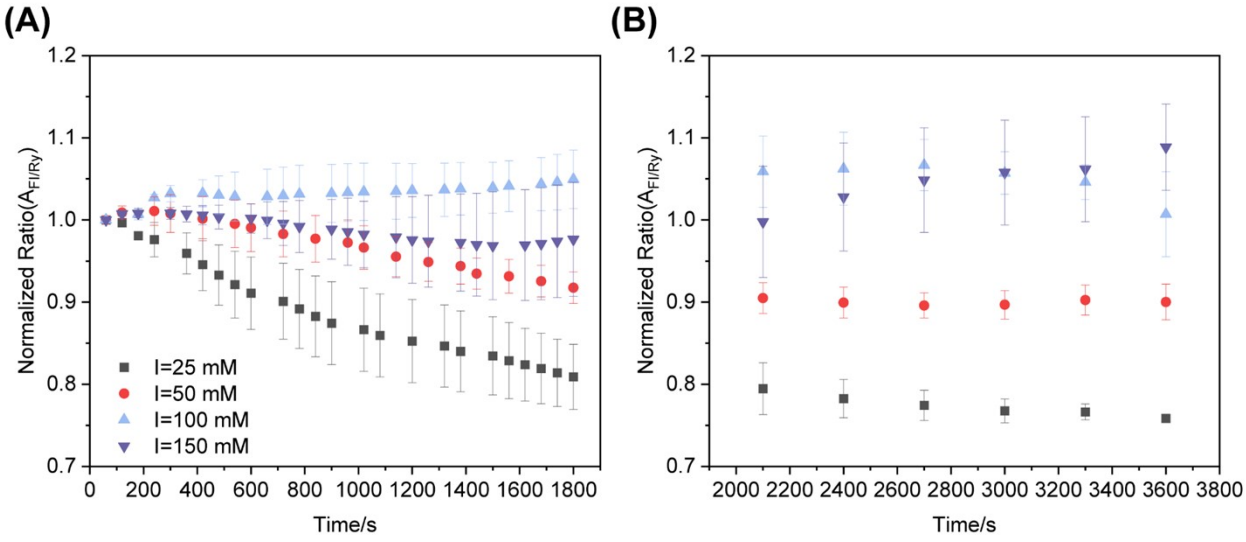

Figure S-6: Plots of normalized $A_{FI/Ry}$ ratio versus time under different ionic strengths: (A) Initial mixing, adsorption, and penetration phase, 0-1800 s., (B) Annealing phase, 1800-3600 s.

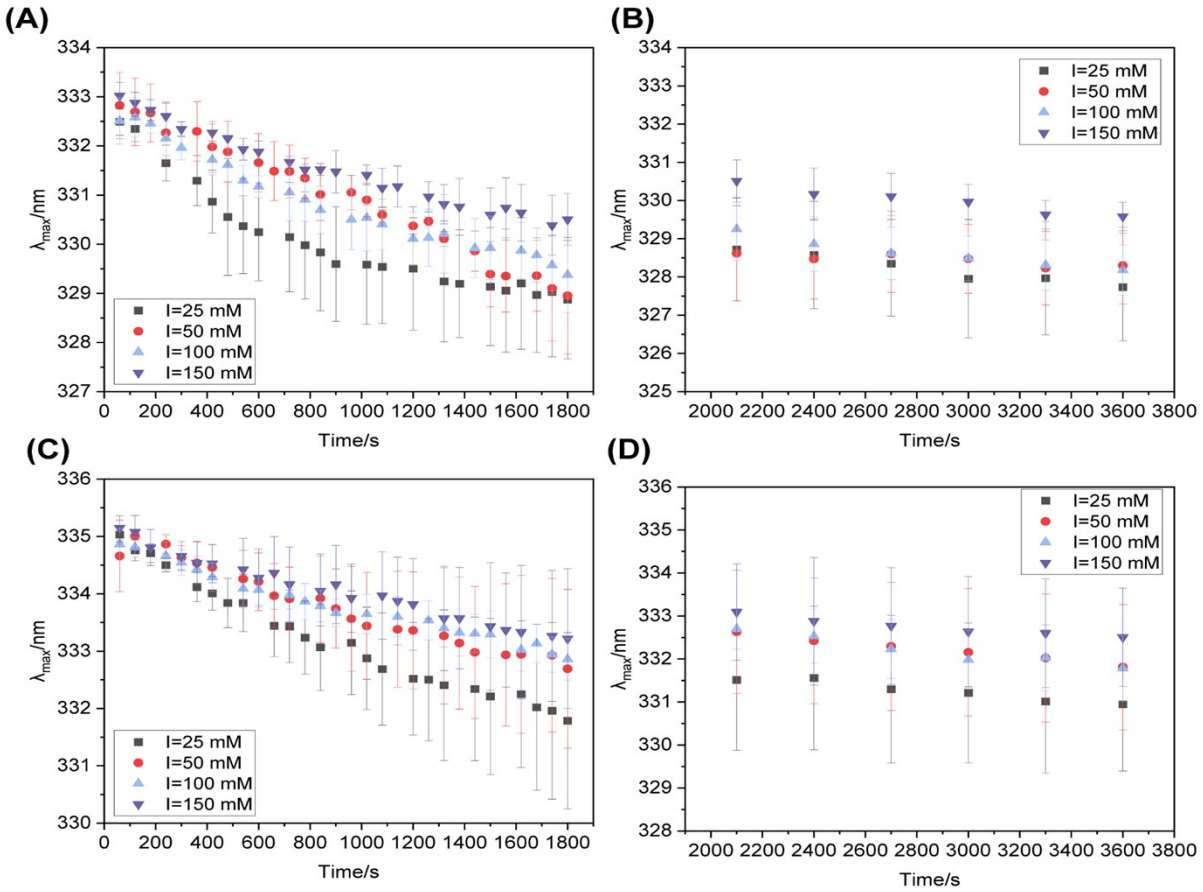

Figure S-7*:* Plots of fluorescence emission maximum wavelength (λ_{max}) versus time under different ionic strengths: (A) 0-1800 s. from VV measurements, (B) 1800-3600 s. from VV measurements; (C) 0-1800 s. from VH measurements, (D) 1800-3600 s. from VH measurements.

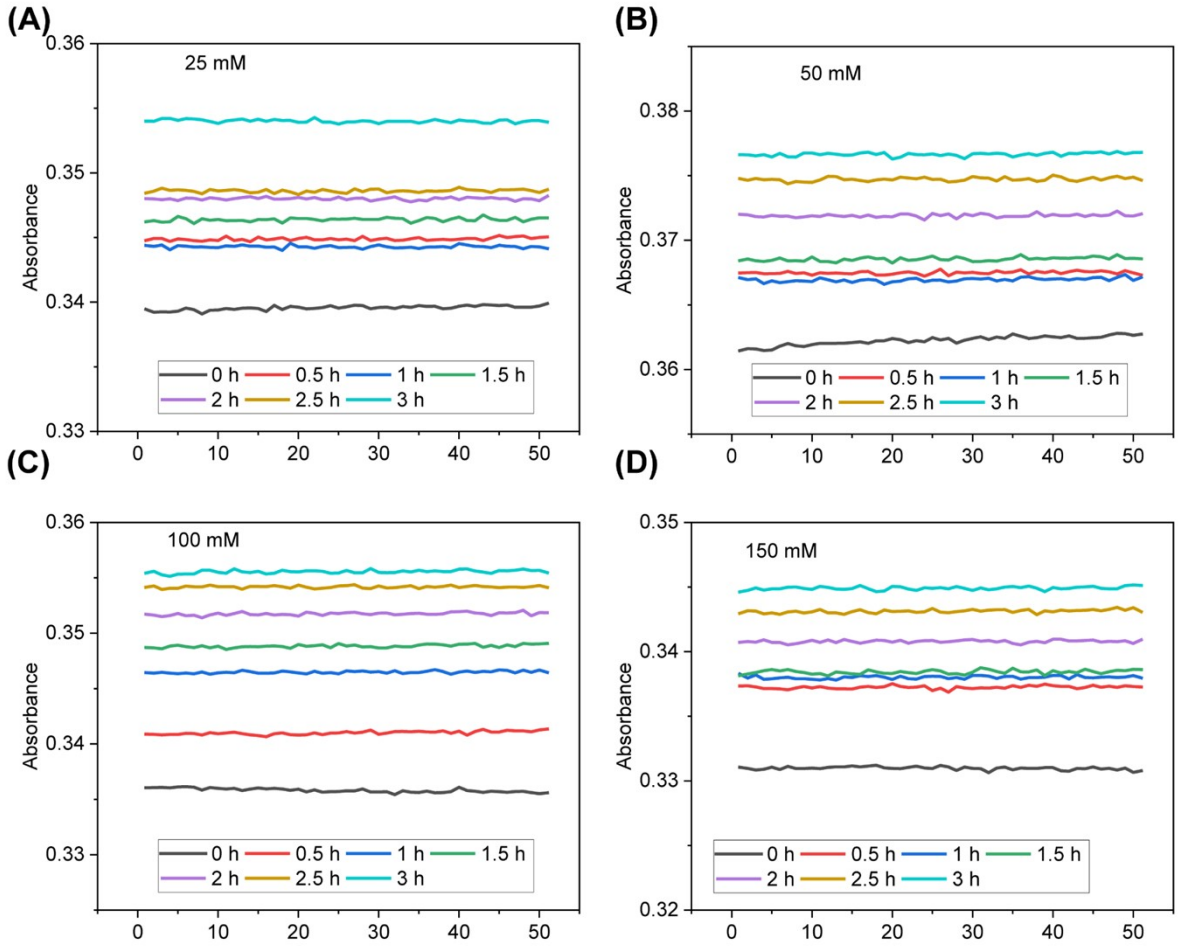

Figure S-8*:* Change in absorbance signals (280 nm) with time after HSA and liposome mixing: (Top) Absorbance stability in different ionic strengths buffers. Data collected from sequential 50 spectral measurements at starting times of : 0 min, 0.5 h, 1 h, 1.5 h, 2 h, 2.5 h, and 3 h after mixing.

Table S-2: Maximum emission wavelength ($\lambda_{max,}$ VH) of HSA and HSA-DMPC Liposome (HSA-DMPC.) complexes at different ionic strengths. $\Delta\lambda_{max}$ is the shift in the maximum emission wavelength for each time interval relative to the preceding interval. For the 0-100s interval this is relative to the free HSA.

λ_{max} (nm)	Ionic strengths			
	25 mM	50 mM	100 mM	150 mM
HSA	335.1 ± 0.6	335.2 ± 0.5	335.0 ± 0.6	335.3 ± 0.5
HSA-DMPC 0-100 s	334.9 ± 0.6	334.8 ± 0.8	334.8 ± 0.6	335.1 ± 0.8
HSA-DMPC 0.5 h	331.8 ± 1.5	332.7 ± 1.4	332.9 ± 0.4	334.1 ± 0.3
HSA-DMPC 1 h	330.9 ± 1.5	331.8 ± 1.5	331.8 ± 0.8	333.3 ± 0.2
HSA-DMPC 3 h	329.0 ± 1.0	330.6 ± 1.9	330.1 ± 0.5	332.1 ± 0.1
$\Delta\lambda_{max}$ (0-100 s)	0.2 ± 0.8	0.4 ± 0.9	0.2 ± 0.8	0.2 ± 0.9
$\Delta\lambda_{max}$ (100 s-0.5 hr.)	**3.1 ± 1.6**	**2.1 ± 1.6**	**1.9 ± 0.7**	**1.0 ± 0.9**
Δ_{max} (0.5 hr-1 hr.)	0.9 ± 2.1	0.9 ± 2.1	1.1 ± 0.9	0.8 ± 0.4
$\Delta\lambda_{max}$ (1 hr-3 hr.)	1.9 ± 1.8	1.2 ± 2.4	1.7 ± 0.9	**1.2 ± 0.2**
$\Delta\lambda_{max}$ (total)	5.9 ± 1.2	4.2 ± 2.1	4.7 ± 0.8	3.0 ± 0.8

1.8 Debye Lengths.

Increasing ionic strength compresses the electrical double layer, thereby reducing electrostatic repulsion and facilitating closer approach of liposomes, which promotes both aggregation and protein adsorption.[7, 8] This phenomenon is quantitatively described by the Debye–Hückel model,[9, 10] which predicts a progressive decrease in the Debye screening length with increasing ionic strength (**Equation S3**).

$$\kappa^{-1} = \frac{0.304}{\sqrt{I(M)}} \qquad \textbf{Equation S3}$$

Calculated Debye lengths were: 1.93 nm at 25 mM, 1.36 nm at 50 mM, 0.96 nm for 100 mM, and 0.78 nm at 150 mM.

1.9 Zeta potential measurements

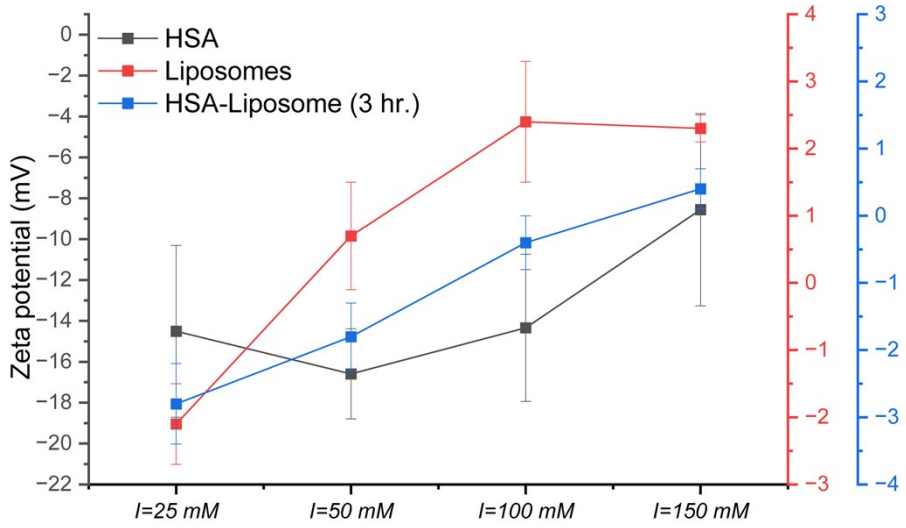

Figure S-9: Zeta potential measurements of HSA, liposomes, and HSA–liposome complexes (after 3 h incubation) at different ionic strengths (I = 25–150 mM). Data are the mean ± SD (n=3).

1.10 Nanoparticle Tracking Analysis (NTA).

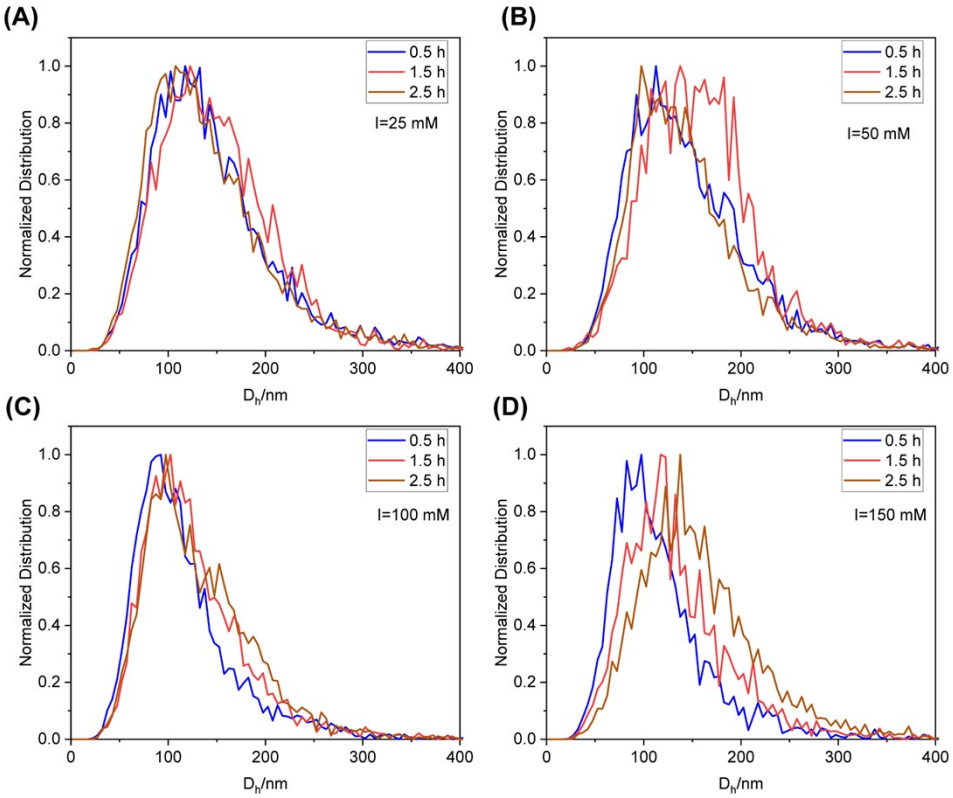

Figure S-10*:* NTA analysis (normalized PSD) of HSA-Liposome (HSA-Lip.) interaction at different times after mixing (0.5, 1.5, and 2.5 hours) under different ionic strengths.

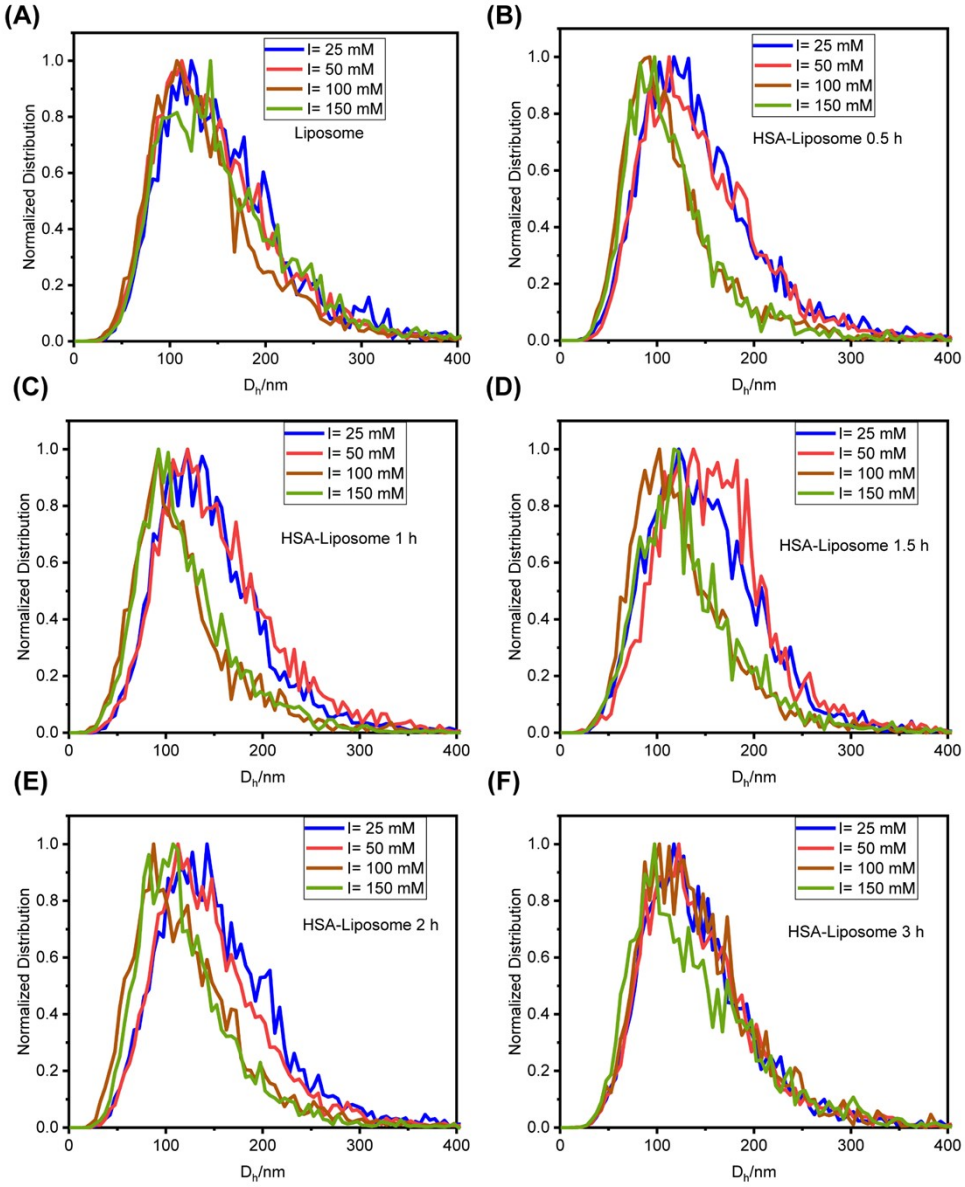

Figure S-11*:* NTA analysis (normalized PSD) of: (A) Liposome as prepared; and at different times after mixing: (B) 30 minutes; (C) 1 hour; (D) 1.5 hours; (E) 2 hours; (F) 3 hours.

Table S-3: NTA size data for HSA–liposome samples as a function of ionic strength (I, mM) and incubation time. Values are reported as mean ± SD (n=5 measurements on same sample aliquot).

Ionic Strength	***samples***	***Time***	***Mode (nm)***	***Mean (nm)***	***D10 (nm)***	***D50 (nm)***	***D90 (nm)***
I=25 mM	***Liposome***	/	119 ***± 8***	157 ***± 3***	85 ***± 4***	143 ***± 3***	241 ***± 11***
	HSA-DMPC	0.5 h	124 ± 16	148 ± 3	80 ± 2	134 ± 2	231 ± 12
		1 h	128 ± 23	147 ± 4	86 ± 2	137 ± 4	218 ± 10
		2 h	138 ± 15	157 ± 5	85 ± 4	144 ± 4	235 ± 14
		3 h	123 ± 15	145 ± 6	80 ± 4	133 ± 5	217 ± 13
I=50 mM	***Liposome***	***/***	118 ± 24	149 ± 3	81 ± 3	137 ± 2	233 ± 11
	HSA-DMPC	0.5 h	120 ± 22	149 ± 6	80 ± 4	136 ± 8	226 ± 9
		1 h	127 ± 20	154 ± 10	86 ± 5	143 ± 7	233 ± 18
		2 h	125 ± 20	147 ± 4	83 ± 4	135 ± 5	221 ± 7
		3 h	122 ± 14	145 ± 4	81 ± 4	133 ± 3	220 ± 6
I=100 mM	***Liposome***	***/***	106 ± 10	140 ± 2	77 ± 3	127 ± 2	224 ± 5
	HSA-DMPC	0.5 h	91 ± 10	117 ± 3	65 ± 2	104 ± 1	187 ± 17
		1 h	96 ± 10	120 ± 4	64 ± 3	106 ± 5	194 ± 9
		2 h	93 ± 7	125 ± 3	63 ± 6	112 ± 4	199 ± 7
		3 h	107 ± 16	143 ± 5	79 ± 4	132 ± 4	221 ± 16
I=150 mM	***Liposome***	***/***	130 ± 16	157 ± 10	83 ± 5	143 ± 11	240 ± 17
	HSA-DMPC	0.5 h	90 ± 8	118 ± 6	66 ± 3	106 ± 5	183 ± 10
		1 h	97 ± 5	122 ± 2	68 ± 2	110 ± 2	190 ± 10
		2 h	99 ± 15	123 ± 5	69 ± 2	111 ± 5	190 ± 9
		3 h	112 ± 34	144 ± 12	72 ± 3	129 ± 12	231 ± 24

1.11 Correlation between $A_{Fl/Ry}$ ratio and particle size.

The mean sizes (number weighted) reported by NTA were different to that extracted from DLS, (Z_{av}, intensity weighted) and this has practical consequences for monitoring protein-liposome reactions in terms of size changes. NTA has better size resolution than DLS for these polydisperse samples (PdI 0.14 to 0.25), providing a truer PSD, and thus the mean size it provides is probably a more accurate size estimate than the Z_{av} from the Cumulants fit of DLS measurements. Direct correlation between NTA and DLS for polydisperse samples was not really feasible,[11] and thus these size models are method and sample specific. A linear correlation (**Figure S12**A) was observed between the normalized $A_{Fl/Ry}$ ratio and D_h (Z_{av}) across all ionic strengths suggests however, for the NTA mean size plots (**Figure S12**B) trends were only apparent for the higher ionic strengths.

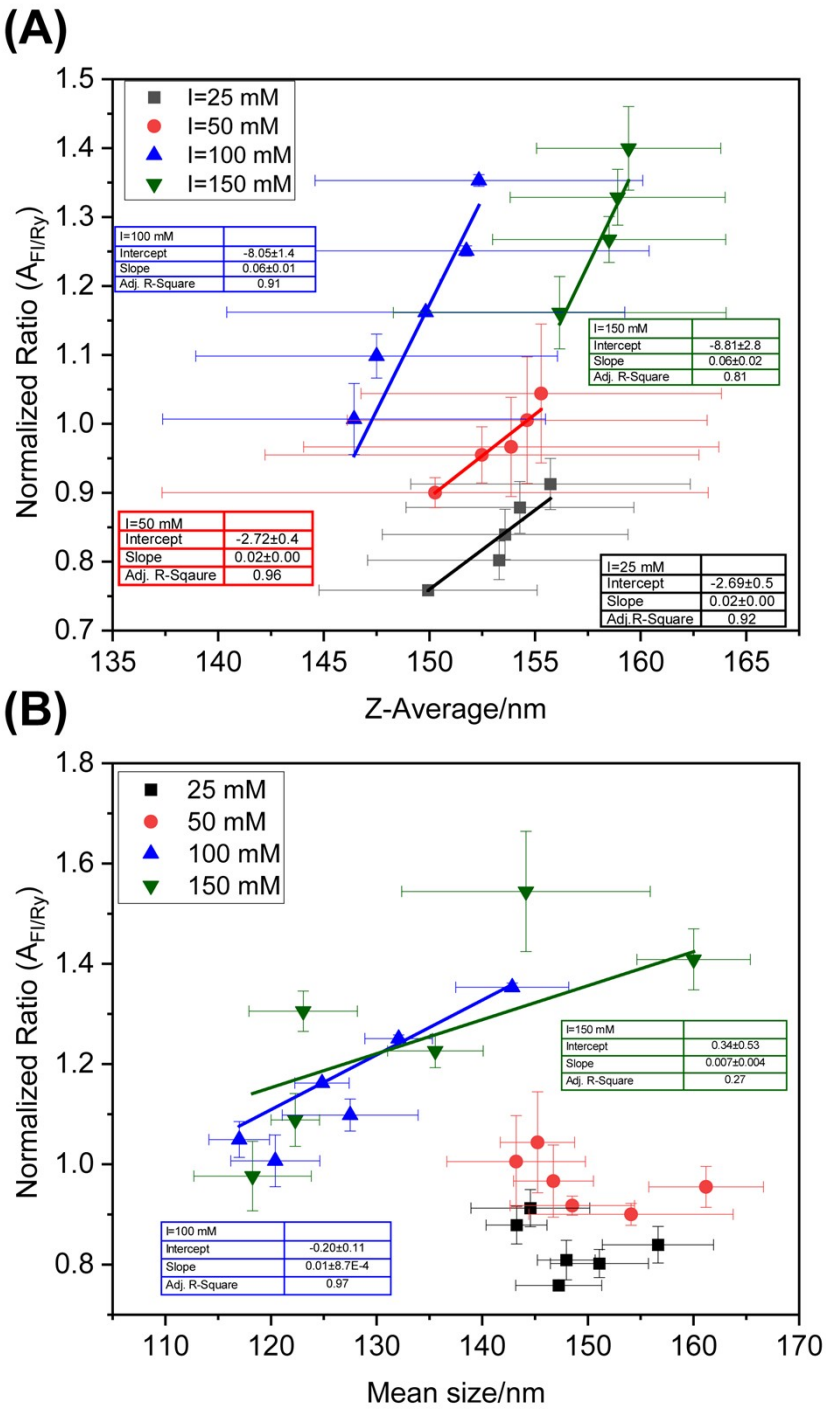

Figure S-12*:* Plot of normalized $A_{FI/Ry}$ ratio versus particle size as measured by: (A) Z-average hydrodynamic diameter from DLS (Cumulants fit) and (B) mean size from NTA.

1.12 Statistical analysis.

This section provides an overall statistical analysis about all DLS and measured spectral parameter datasets acquired during the different experimental stages, including liposomes in buffer, initial mixing and adsorption (0–200 s), and Penetration Phase （up to 30 minutes）and Protein corona growth/evolution (0.5h-3 h). Depending

on the experimental design, one-way or two-way analysis of variance (ANOVA) was used to evaluate the effects of ionic strength, incubation time, and their interaction. Where significant effects were identified, appropriate post hoc multiple-comparison tests were applied to determine differences between individual conditions. Tukey's test [12] was used for comparisons among multiple ionic-strength conditions, whereas Šídák's test [13] was applied for planned comparisons between time points within each ionic-strength group, and Dunnett's multiple-comparisons test [14] because the analysis was designed around comparisons with predefined reference conditions rather than all possible pairwise comparisons. Specifically, APIES-derived and DLS-derived values at each incubation time were compared to the situation at 30 minutes after mixing within a given ionic strength. Statistical significance was defined at $\alpha = 0.05$.

Liposomes in Buffer

ANOVA followed by Tukey's multiple-comparison test of the Peak 1 DLS data show that the apparent increase in liposome size with ionic strength was not statistically significant ($p > 0.05$). In particular, the difference between 100 mM and 150 mM was not significant ($p = 0.3148$).

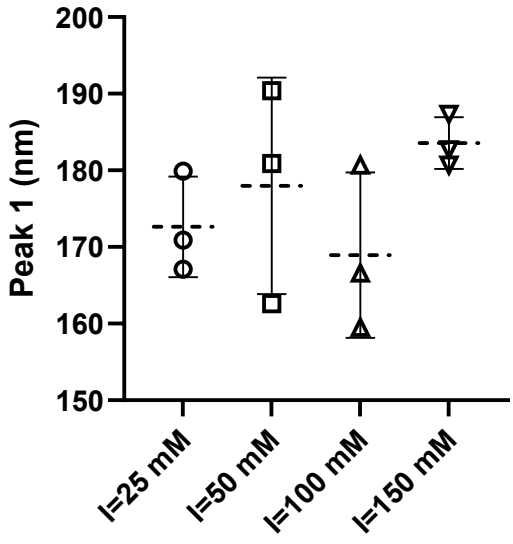

Figure S13*:* ANOVA analysis of liposome size (Peak 1 from the distribution fit) measured under different ionic strength conditions .

DLS Initial mixing and adsorption （0-200 s.）:

All DLS data (Z-average and Peak 1) were analysed using a two-way analysis of variance (ANOVA) to evaluate the effects of **time** (t_o vs t_{200}) and **ionic strength** (25, 50, 100, and 150 mM). Statistical significance was defined at $\alpha = 0.05$. When appropriate, Šídák's multiple comparisons test was applied to assess differences between time points within each ionic strength condition (**Figure S14**), as this method controls the family-wise error rate while providing greater statistical power than the more conservative Bonferroni correction when only a limited number of planned pairwise comparisons are performed.

Two-way ANOVA showed a significant main effect of time for both Z-average and Peak 1, indicating systematic changes between t_o and t_{200} (Z-average: $P = 0.0002$; Peak 1: $P = 0.0008$).

For Z-average, ionic strength also had a significant main effect (P = 0.0102), whereas the interaction between time and ionic strength was not significant (P > 0.45). Post hoc Šídák comparisons nevertheless indicated that the decrease from t_o to t_{200} was significant at 25 and 50 mM, but not at 100 or 150 mM.

For Peak 1, ionic strength had no significant main effect (P = 0.1832), and there was likewise no interaction between time and ionic strength (P > 0.45), indicating that the temporal change was broadly independent of ionic strength. Post hoc analysis showed that the difference between t_o and t_{200} reached statistical significance only at 25 mM.

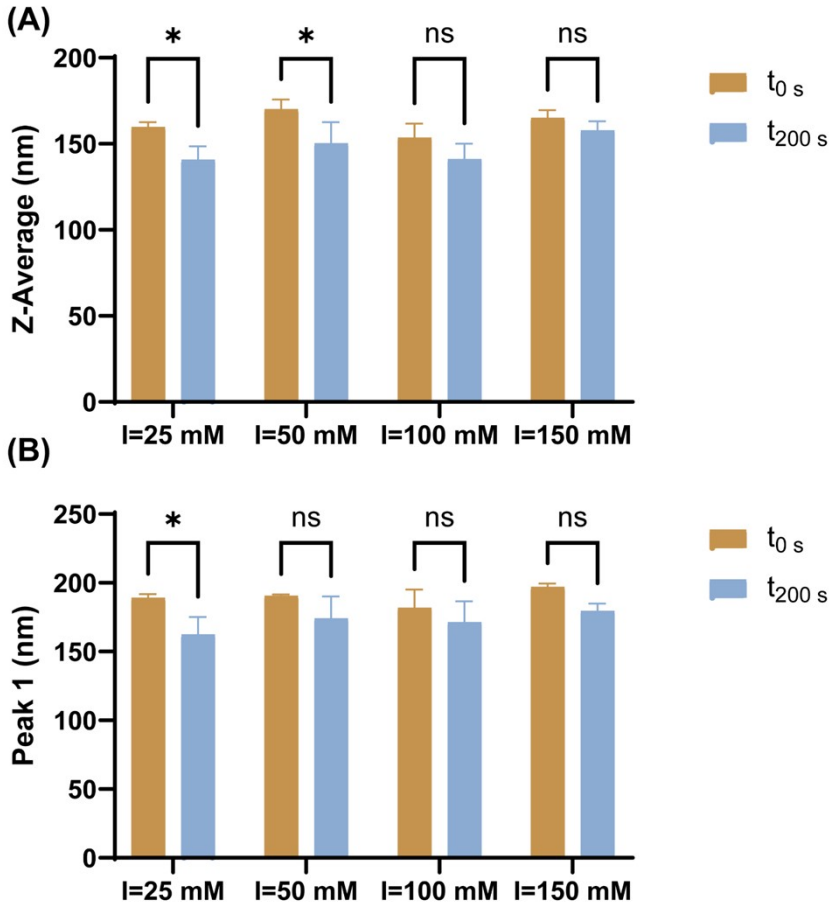

Figure S14*:* ANOVA analysis of DLS data (0-200 s time range) related to HSA-liposome size changes in the different buffers, (A) Z-Average size (Cumulants fit), (B) Peak 1 (Distribution fit).

DLS Penetration Phase （up to 30 minutes）

The effects of time (t_o vs t30 min) and ionic strength (25, 50, 100, and 150 mM) were analysed using the same two-way ANOVA and Šídák multiple-comparisons procedure described above.

Two-way ANOVA revealed a significant main effect of time on Z-average (P = 0.0009), indicating an overall change between t_o and $t_{30\ min}$ across all ionic strength conditions. Ionic strength also exerted a significant main effect (P = 0.0461), whereas the interaction between time and ionic strength was not significant (P > 0.45). Post hoc Šídák multiple-comparisons analysis showed that the reduction in Z-average between t_o and t30 min reached statistical significance only at 50 mM (P = 0.0102).

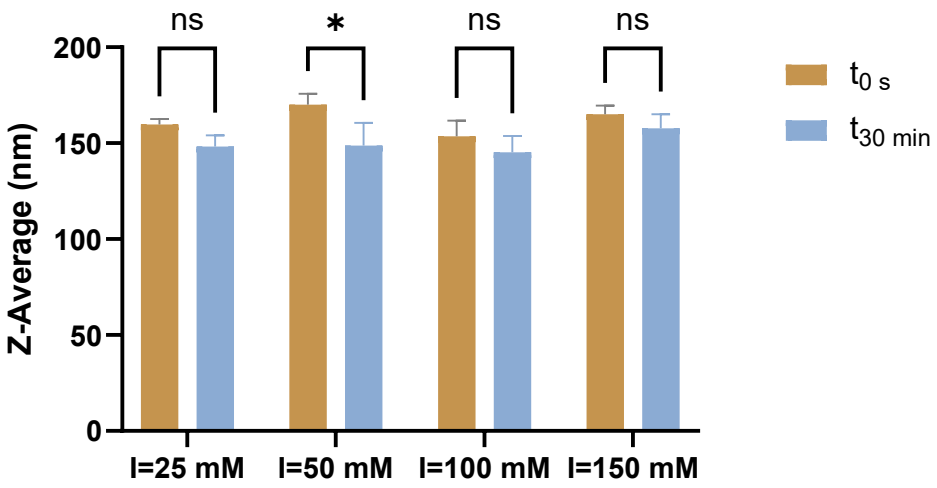

Figure S15*:* ANOVA analysis of Z-Average size data (0-30 minute time range) related to HSA-liposome size changes under different ionic strengths.

DLS Protein corona growth/evolution

Two-way ANOVA (**Figure S16**) was used to assess the effects of ionic strength (25–150 mM) and incubation time (0.5–3 h) on the particle size (Z-Average). This revealed a significant effect of the time factor (P = 0.0264). Post hoc comparisons were conducted using Dunnett's test [14]. When comparing time points (vs. 0.5 h) within each ionic strength, there were no significant differences between individual groups.

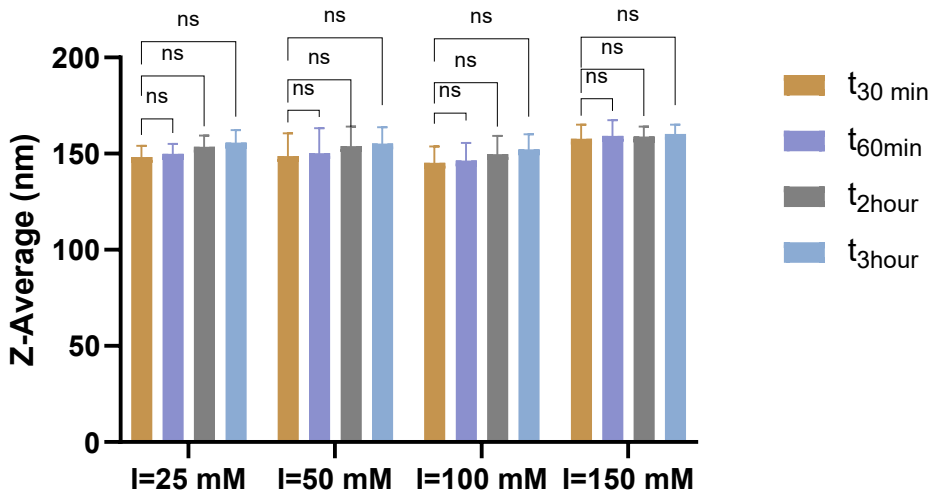

Figure S16*:* ANOVA analysis of Z-Average intensity under different incubation time and ionic strength conditions.

APIES Initial mixing and adsorption （0-200 s.）:

The PIE data (normalized ratio($A_{FI/Ry}$), normalized fluorescence intensity, and emission maximum (λ_{max}) were analysed by two-way ANOVA using time and ionic strength as factors.

Normalized $A_{FI/Ry}$ ratio (Figure S17 A) showed a significant between time and ionic strengths (P = 0.0013), indicating that the effect of time depended on the ionic strengths. The main effect of ionic strengths was also significant (P = 0.0013), whereas the overall main effect of time was not significant (P = 0.2024).

Post hoc Šídák multiple comparisons were performed to compare t_os and t_{200}s within each ionic strength. A significant decrease in the normalized $A_{FI/Ry}$ ratio was observed only at 25 mM (p = 0.0011), whereas no significant changes were detected at 50 mM (p = 0.8167), 100 mM (p = 0.2758), or 150 mM (p = 0.7581). These results indicate that the time-dependent decrease in the AFI/Ry ratio occurred only under the lowest ionic strength condition.

For Normalized Fluorescence intensity (Figure S17 B), two-way ANOVA showed a highly significant main effect of time ($p < 0.0001$), indicating an overall decrease in fluorescence intensity from t_o to t_{200}. Neither the interaction between time and ionic strength nor the main effect of ionic strength reached significance (both p = 0.0540), although both values were close to the significance threshold. Thus, the decrease in fluorescence intensity was broadly similar across all ionic strengths. Šídák post hoc comparisons confirmed significant decreases between t_o and t_{200} at all ionic strengths (all $p < 0.0001$).

For λ_{max} (Figure S17 C), two-way ANOVA revealed no significant interaction between time and ionic strength (p = 0.3949) and no significant main effect of ionic strength (p = 0.8145), indicating that λ_{max} did not differ among the buffer conditions and that any temporal trend was similar across ionic strengths. Although a small but significant main effect of time was detected (p = 0.0403). Šídák post hoc comparisons showed no significant change between t_o and t_{200} within any individual ionic strength condition. Therefore, λ_{max} remained essentially unchanged during the first 200 s.

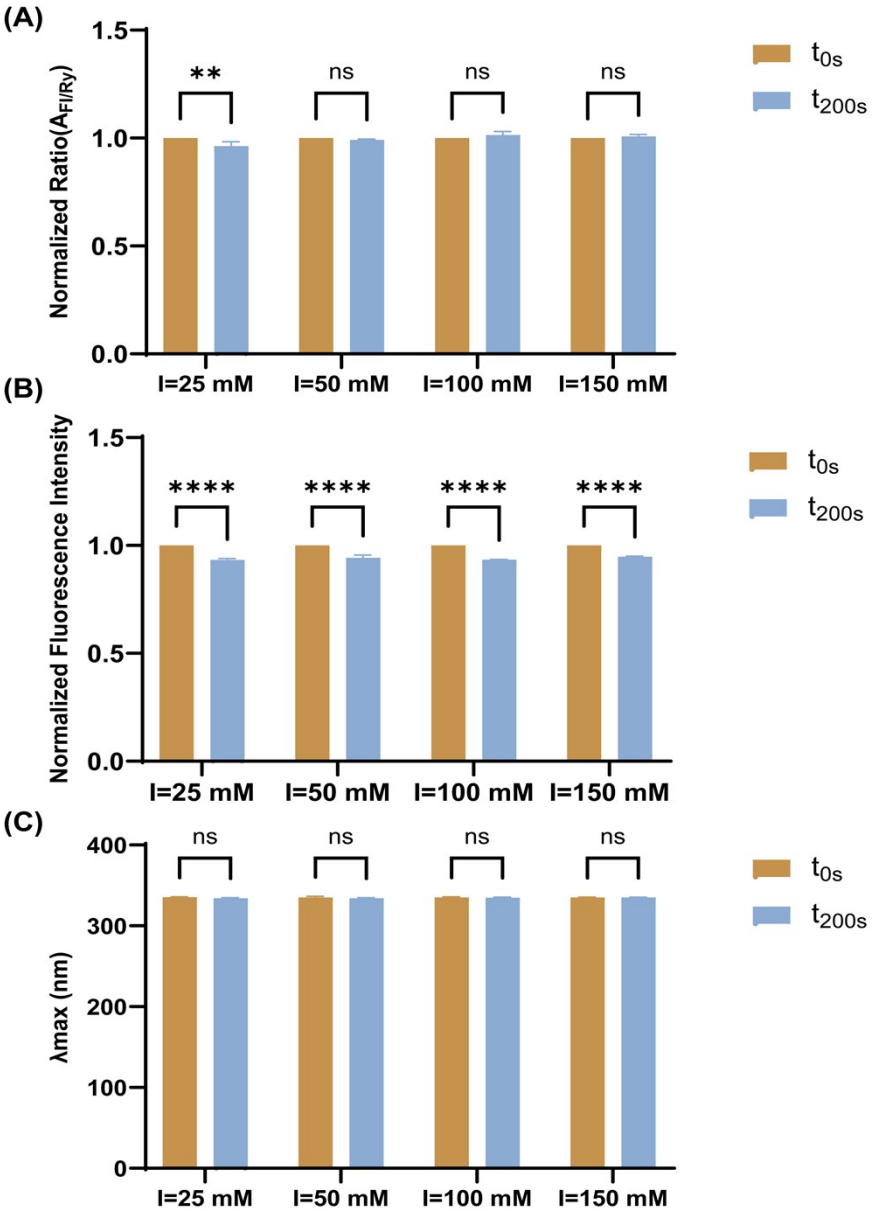

Figure S17*:* ANOVA analysis of measured spectral parameters (0-200 s time range) from HSA-liposome mixtures in different buffers: (A) Normalized $A_{Fl/Ry}$ ratio; (B) Normalized Fluorescence intensity; (C) Emission maximum, λ_{max}.

APIES Penetration Phase （up to 30 minutes）

For the normalized $A_{Fl/Ry}$ ratio (Figure S18 A), two-way ANOVA revealed a significant interaction between time and ionic strength ($p < 0.0001$), indicating that the time-dependent response differed among the ionic strength conditions. Both the main effect of ionic strength ($p < 0.0001$) and the main effect of time ($p = 0.0002$) were also significant. Šídák post hoc comparisons showed that the normalized $A_{Fl/Ry}$ ratio decreased significantly from 0 s to 0.5 h at 25 mM ($p < 0.0001$) and 50 mM ($p = 0.0225$), whereas no significant change was observed at 100 or 150 mM. Thus, the initial decrease in normalized $A_{Fl/Ry}$ ratio occurred only under low-ionic-strength conditions.

For λ_{max} (Figure S18 B), two-way ANOVA showed no significant interaction between time and ionic strength ($p = 0.4353$) and no significant main effect of ionic strength ($p = 0.1046$), indicating that the

change in λ_{max} with time was similar across all ionic strengths. However, there was a significant main effect of time ($p < 0.0001$), demonstrating an overall decrease in λ_{max} from t_0 to 30 minutes. Šídák post hoc comparisons confirmed that this decrease was significant at all ionic strengths: 25 mM ($p < 0.0001$), 50 mM ($p < 0.0001$), 100 mM ($p = 0.0004$), and 150 mM ($p = 0.0033$). Therefore, λ_{max} decreased significantly during the first 30 minutes irrespective of ionic strength.

Similarly, for normalized fluorescence intensity (Figure S18 C), two-way ANOVA showed no significant interaction between time and ionic strength ($p = 0.6424$) and no significant main effect of ionic strength ($p = 0.6424$), indicating that fluorescence intensity changed similarly under all buffer conditions. In contrast, the main effect of time was highly significant ($p < 0.0001$), indicating an overall decrease in fluorescence intensity from 0 s to 0.5 h. Šídák post hoc comparisons confirmed significant decreases at all ionic strengths: 25 mM ($p = 0.0011$), 50 mM ($p = 0.0015$), 100 mM ($p = 0.0305$), and 150 mM ($p = 0.0093$). Thus, normalized fluorescence intensity decreased significantly during the first 30 minutes under all conditions, with no evidence that the magnitude of the decrease depended on ionic strength.

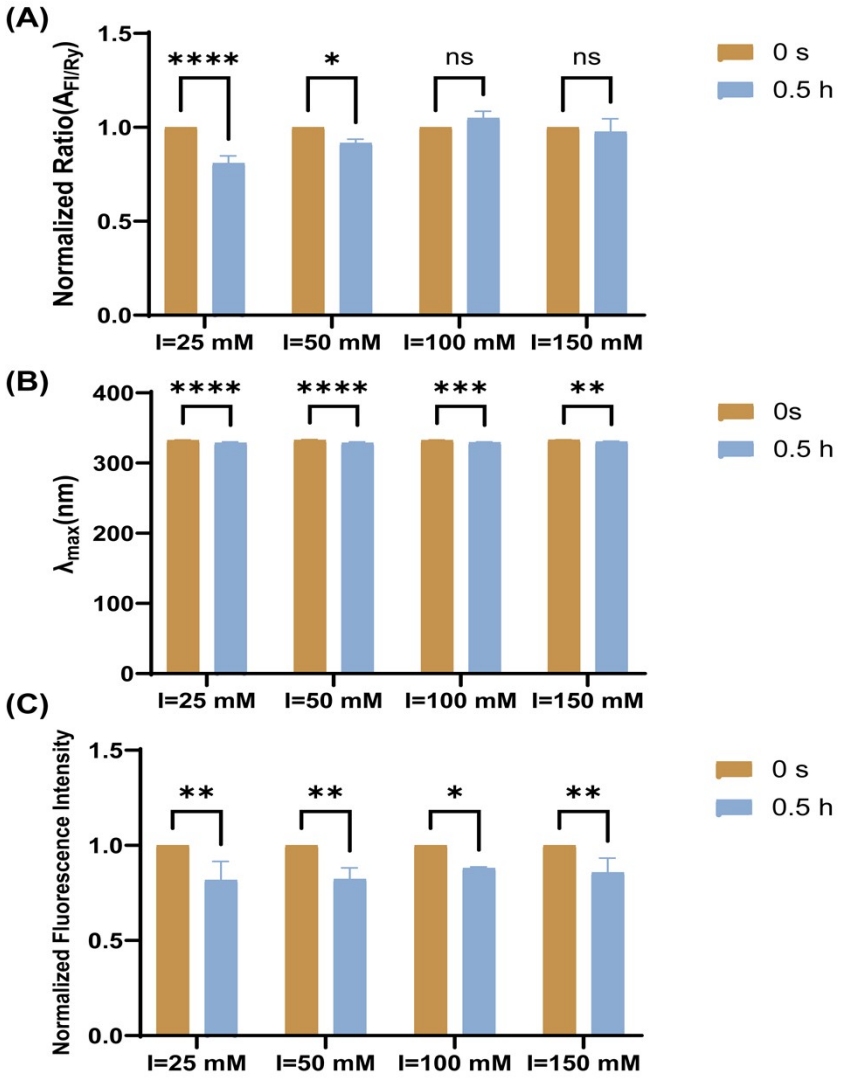

Figure S18*:* ANOVA analysis of measured spectral parameters under different incubation time (0.5 h vs. 0 s) and ionic strength conditions: (A) normalized $A_{FI/Ry}$ ratio, (B) Emission maximum, λ_{max}, (C) Normalized Fluorescence intensity.

APIES Protein corona growth/evolution:

Two-way ANOVA was used to assess the effects of ionic strength (25–150 mM) and incubation time (0.5–3 h) on the normalized $A_{FI/Ry}$ ratio (**Figure S19** A & B).

No significant interaction between ionic strength and time was observed ($p = 0.2280$), indicating that the temporal changes in fluorescence were consistent across ionic strengths. In contrast, both main effects were highly significant, with normalized $A_{FI/Ry}$ ratio varying across ionic strengths ($p < 0.0001$) and over time ($p < 0.0001$). Notably, ionic strength accounted for the largest proportion of variance (70.10%), suggesting it was the dominant factor influencing $A_{FI/Ry}$ ratio. Post hoc comparisons were conducted using Dunnett's test. When comparing time points within each ionic strength (vs. 0.5 h), no significant differences were observed at lower ionic strengths (25 and 50 mM), whereas significant increases at later time points were detected at higher ionic strengths (100 and 150 mM). Conversely, when comparing ionic strengths within each time point (vs. 25 mM), normalized $A_{FI/Ry}$ ratio was significantly higher at 100 and 150 mM across most time points, while differences between 25 and 50 mM were not significant.

For normalized fluorescence intensity (**Figure S19**C), two-way ANOVA likewise showed no significant interaction between ionic strength and time ($p = 0.9690$), indicating that the time-dependent trend was similar at all ionic strengths. Nevertheless, both the main effect of ionic strength ($p = 0.0139$) and the main effect of time ($p < 0.0001$) were significant. Because there was no interaction, the effect of time can be interpreted independently of ionic strength. Overall, normalized fluorescence intensity increased gradually from 0.5 to 3 h.

Dunnett's post hoc analysis showed that, relative to 0.5 h, no significant changes in normalized fluorescence intensity occurred for 25 or 150 mM. For 50 mM, the intensity at 3 hours was significantly higher than at 0.5 h (adjusted $p = 0.0034$), and a similar increase was observed at 100 mM (adjusted $p = 0.0394$). These results indicate a modest but progressive increase in fluorescence intensity during incubation, particularly at intermediate ionic strengths.

For λ_{max} (**Figure S19**D), two-way ANOVA again revealed no significant interaction between ionic strength and time ($p > 0.9999$), indicating that the temporal trend in λ_{max} was similar under all ionic strength conditions. However, both the main effect of ionic strength ($p < 0.0001$) and the main effect of time ($p < 0.0001$) were significant. Overall, λ_{max} remained relatively constant during the first 2 h and then decreased slightly between 2.5 and 3 h.

Dunnett's post hoc comparisons (using 0.5 h as the reference) showed that at 25 mM, λ_{max} decreased significantly at 2.5 h (adjusted $p = 0.0464$) and 3 h (adjusted $p = 0.0140$). For 50 mM and 100 mM, significant increases were observed only at 3 hours (adjusted $p = 0.0478$; and adjusted $p = 0.0262$, respectively). No significant changes were detected for 150 mM. Thus, the increase in λ_{max} after prolonged incubation was greatest at lower ionic strengths, whereas λ_{max} remained essentially unchanged at 150 mM.

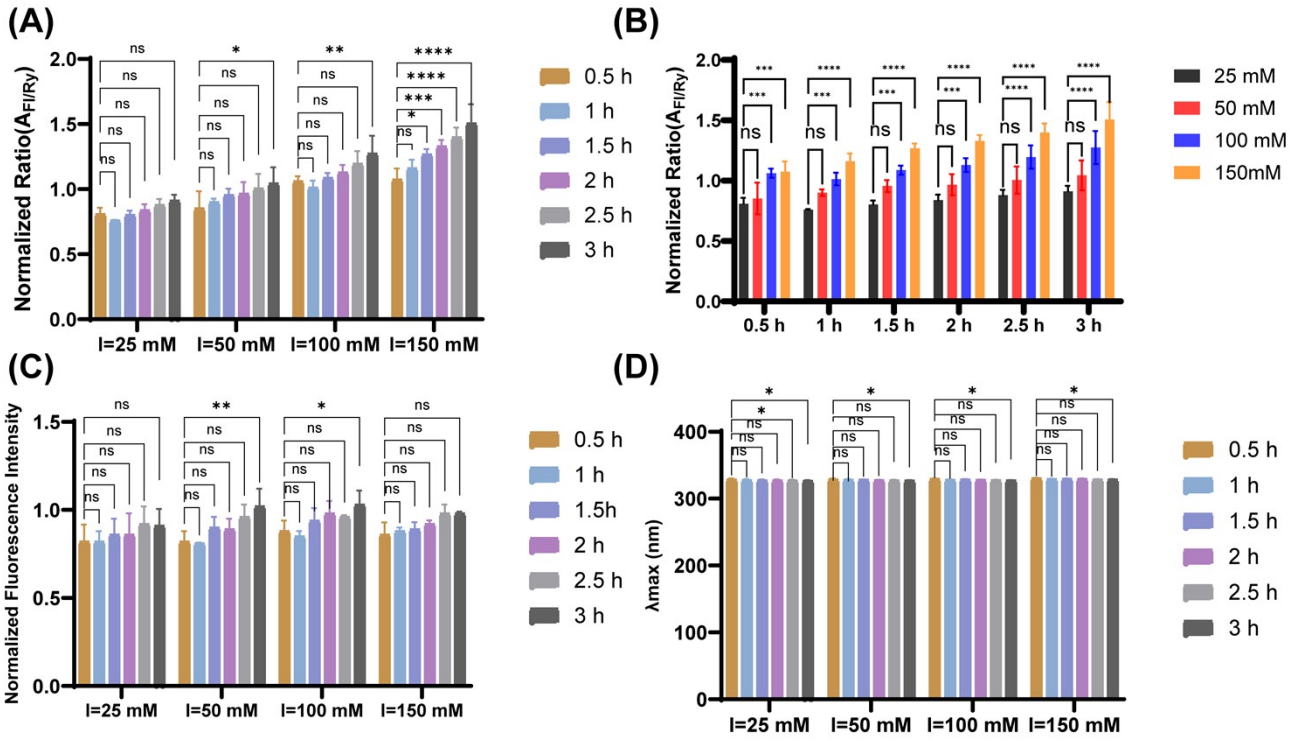

Figure S-19*:* ANOVA analysis of measured spectral parameters under different incubation times (0.5 h-3 h) and ionic strength conditions: (A & B) normalized $A_{FI/Ry}$ ratio, (C) Normalized Fluorescence intensity, (D) Emission maximum, λ_{max}.

Table S-4:. Summary of measured parameter change significance with temporal and ionic strength effects.

Stage	Parameter	Ionic strength （mM）			
		25	**50**	**100**	**150**
200s compared to T_0	Z-Average size	**Yes**	**Yes**	*No*	*No*
	$A_{FI/Ry}$ ratio	**Yes**	*No*	*No*	*No*
	λ_{max}	*No*	*No*	*No*	*No*
	Fluorescence Intensity	**Yes**	**Yes**	**Yes**	**Yes**
30 min compared to T_0	Z-Average size	*No*	**Yes**	*No*	*No*
	$A_{FI/Ry}$ ratio	**Yes**	**Yes**	*No*	*No*
	λ_{max}	**Yes**	**Yes**	**Yes**	**Yes**
	Fluorescence Intensity	**Yes**	**Yes**	**Yes**	**Yes**
3 hours compared to 30 minutes	Z-Average size	*No*	*No*	*No*	*No*
	$A_{FI/Ry}$ ratio	*No*	**Yes**	**Yes**	**Yes**
	λ_{max}	**Yes**	**Yes**	**Yes**	**Yes**
	Fluorescence Intensity	*No*	**Yes**	**Yes**	*No*

a. High resolution Figure 2 plots:

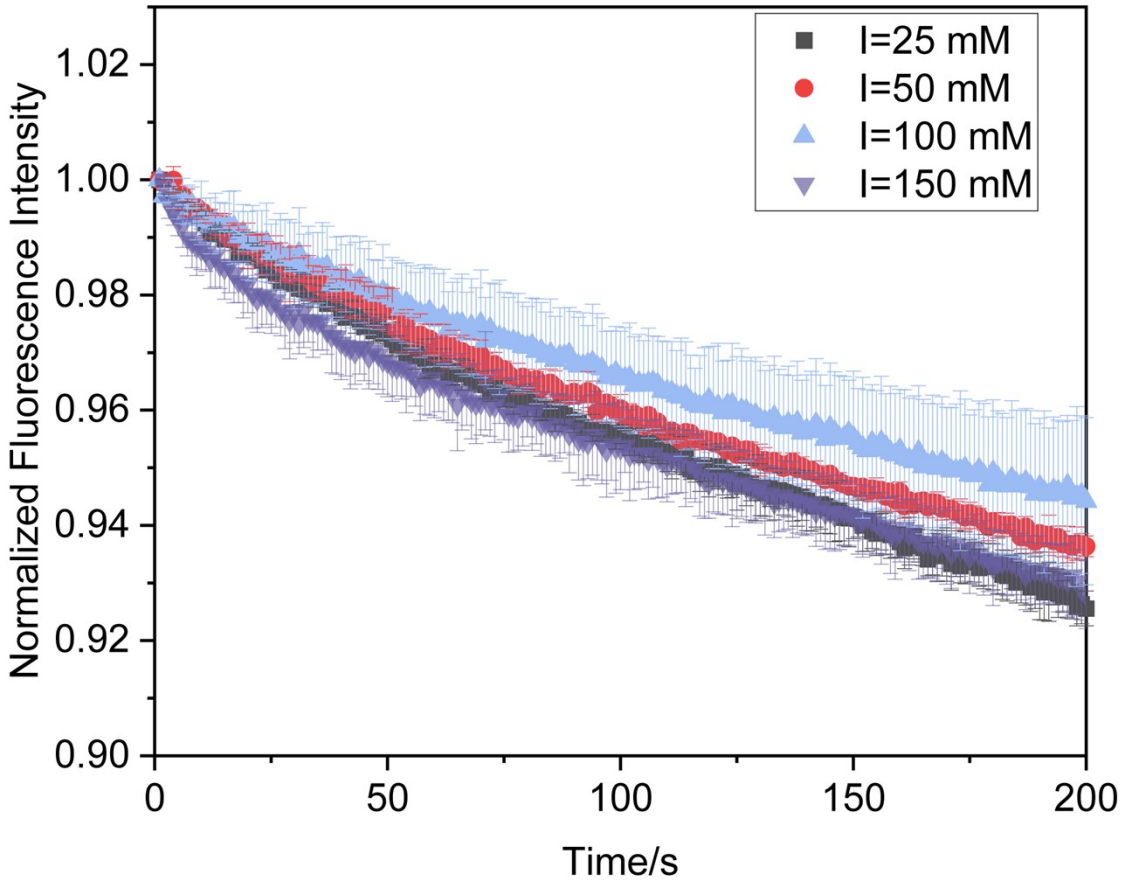

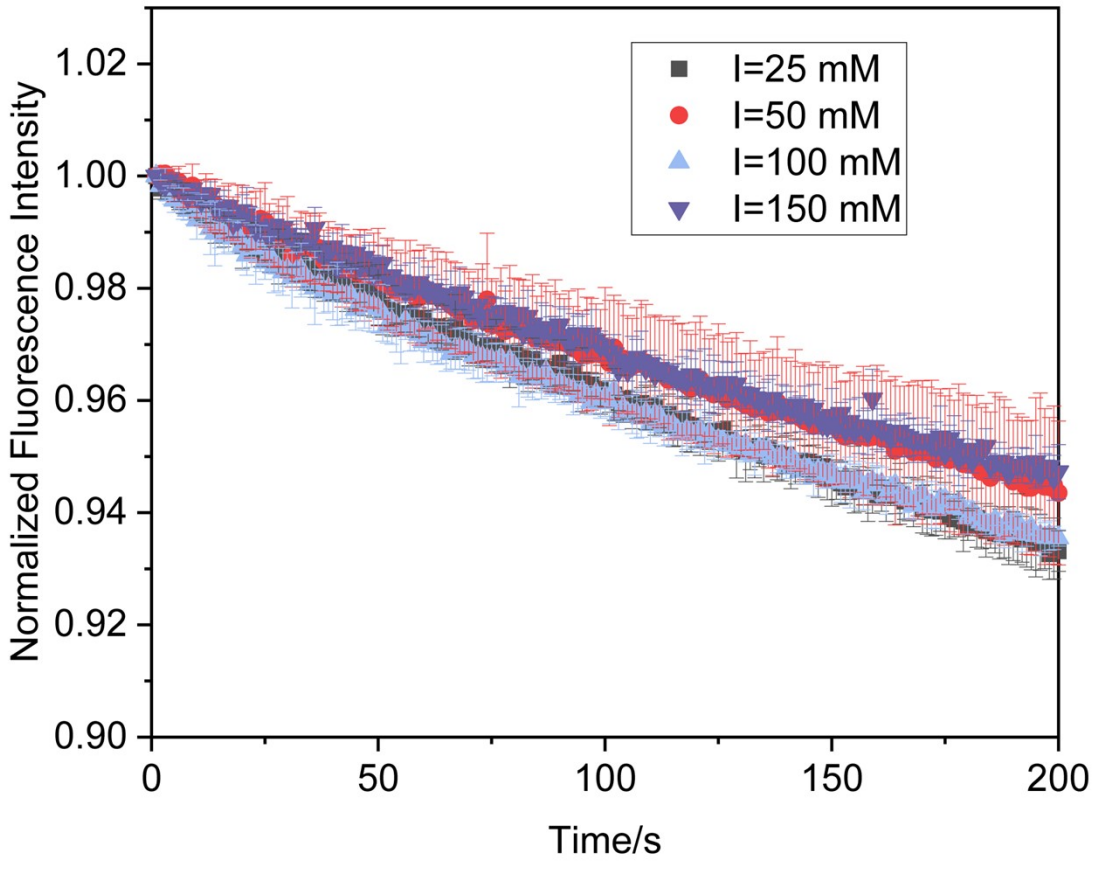

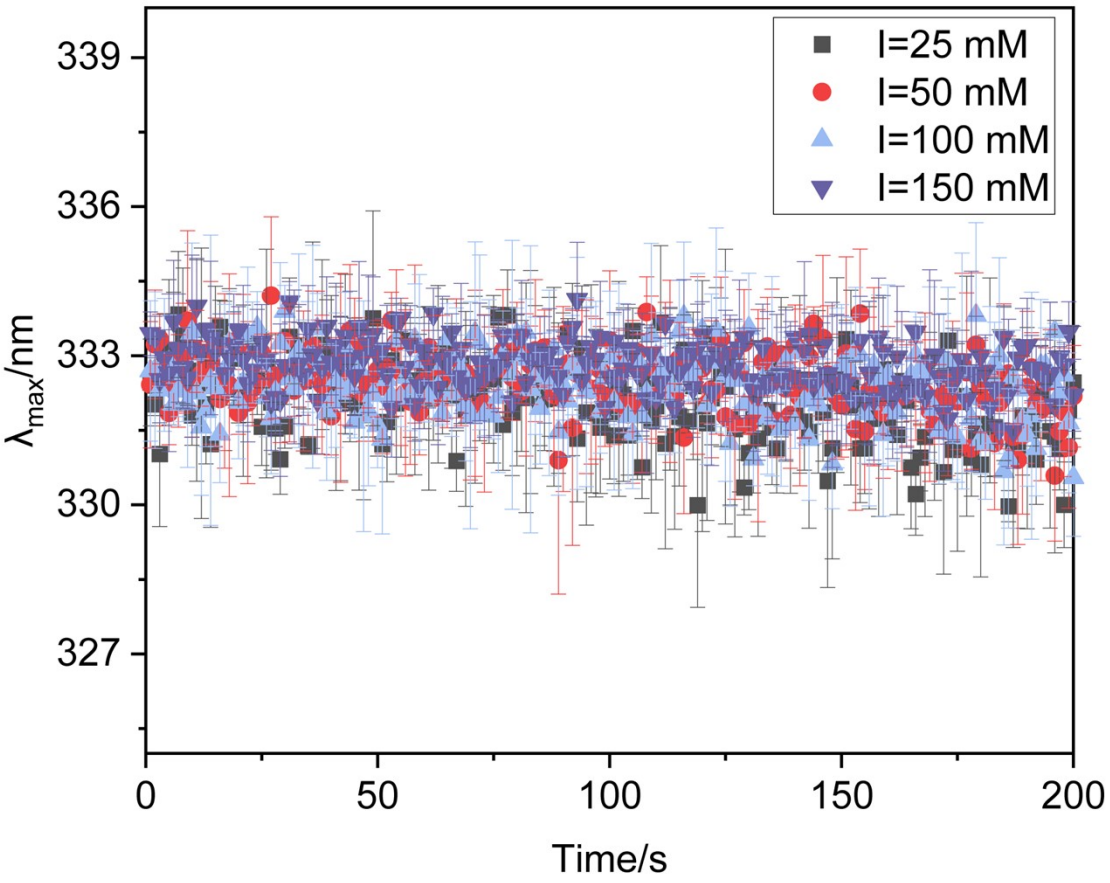
I=25 mM
I=50 mM
I=100 mM
I=150 mM
339
336
333
330
327
λmax/nm
0
50
100
150
200
Time/s

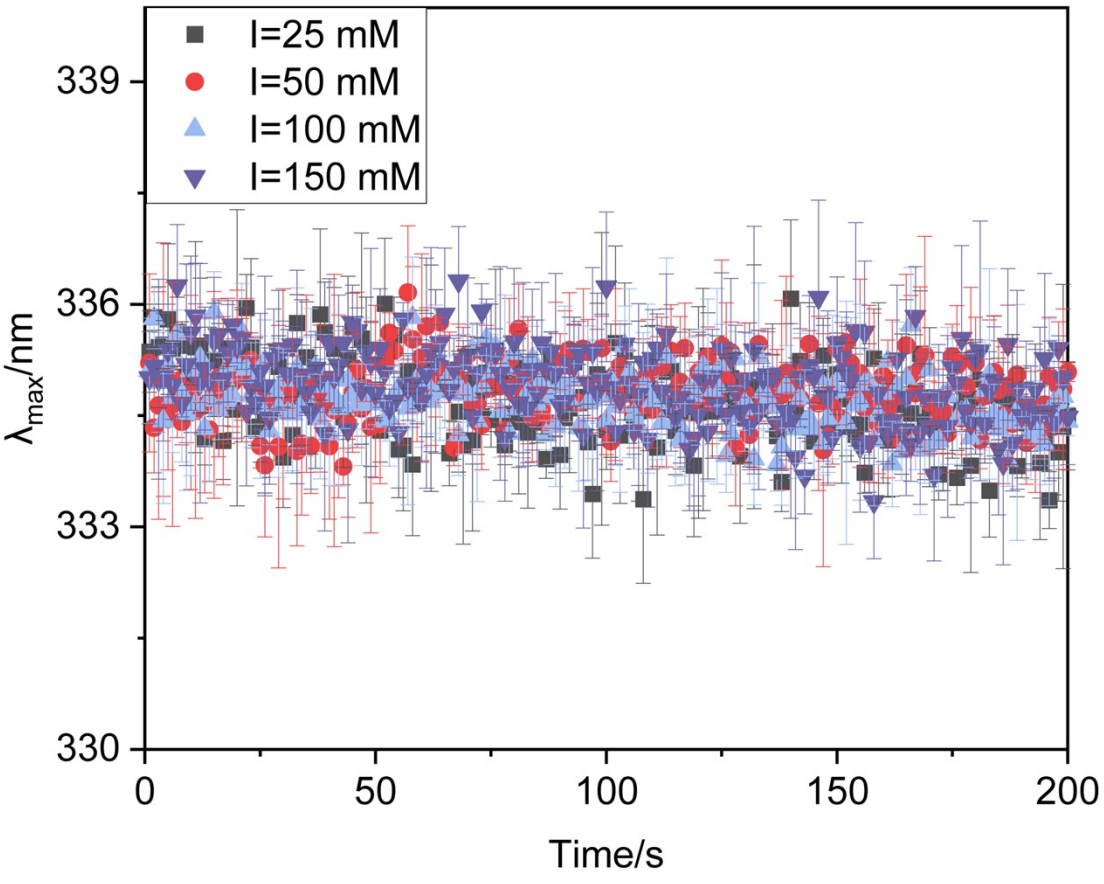
I=25 mM
I=50 mM
I=100 mM
I=150 mM
339
336
333
330
λmax/nm
0
50
100
150
200
Time/s

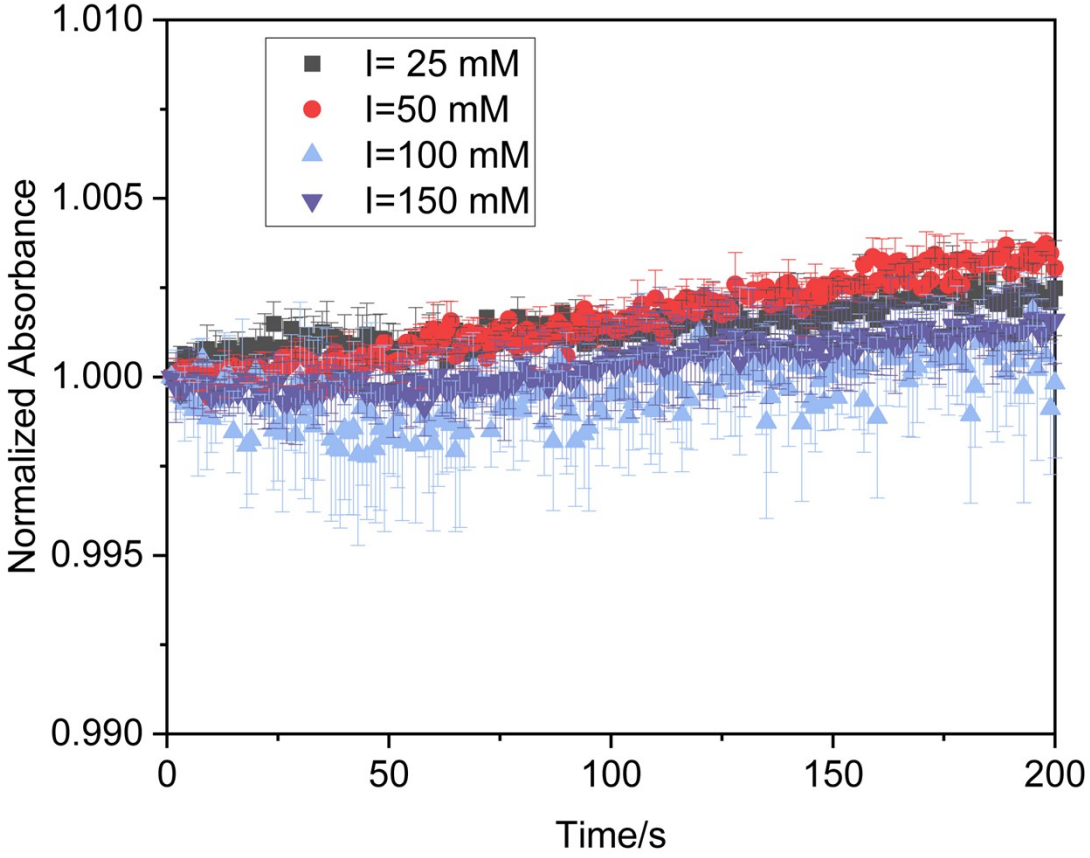
1.010
1.005
1.000
0.995
0.990
Normalized Absorbance
I= 25 mM
I=50 mM
I=100 mM
I=150 mM
0
50
100
150
200
Time/s

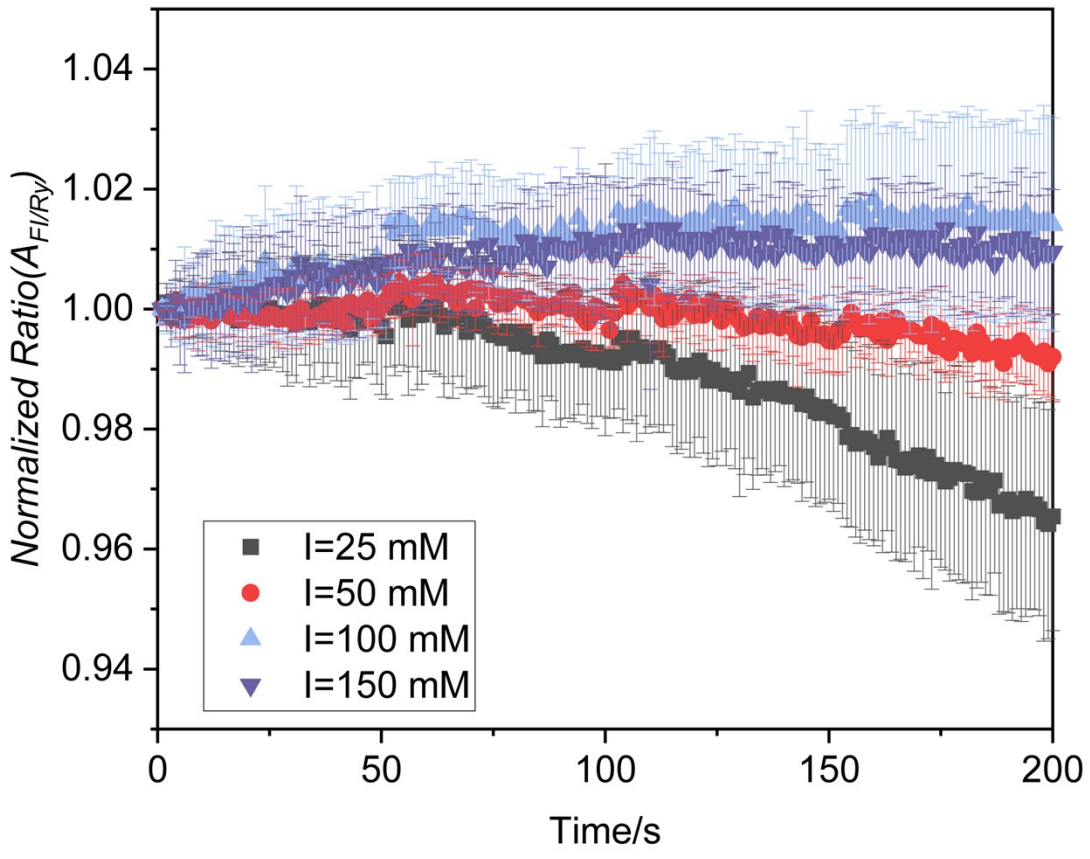
1.04
1.02
1.00
0.98
0.96
0.94
Normalized Ratio($A_{FI/Ry}$)
I=25 mM
I=50 mM
I=100 mM
I=150 mM
0
50
100
150
200
Time/s

References.

1. He, X.M. and D.C. Carter, *Atomic structure and chemistry of human serum albumin.* Nature, 1992. **358**(6383): p. 209-215.

2. M, H., E.A. Azzazy, and R.H. Christenson, *All About Albumin: Biochemistry, Genetics, and Medical Applications. Theodore Peters, Jr. San Diego, CA: Academic Press, 1996, 432 pp, $85.00. ISBN 0-12-552110-3.* Clinical Chemistry, 1997. **43**.

3. Celedón, G., et al., *Effect of Human Serum Albumin Upon the Permeabilizing Activity of Sticholysin II, a Pore Forming Toxin from Stichodactyla heliantus.* The Protein Journal, 2013. **32**(8): p. 593-600.

4. Mozafari, M., E. Mazaheri, and K. Dormiani, *Simple equations pertaining to the particle number and surface area of metallic, polymeric, lipidic and vesicular nanocarriers.* Scientia pharmaceutica, 2021. **89**(2): p. 15.

5. Gordon, F., Y. Casamayou-Boucau, and A.G. Ryder, *Evaluating the interaction of human serum albumin (HSA) and 1, 2-dimyristoyl-sn-glycero-3-phosphocholine (DMPC) liposomes in different aqueous environments using anisotropy resolved multi-dimensional emission spectroscopy (ARMES).* Colloids and Surfaces B: Biointerfaces, 2022. **211**: p. 112310.

6. Stetefeld, J., S.A. McKenna, and T.R. Patel, *Dynamic light scattering: a practical guide and applications in biomedical sciences.* Biophysical Reviews, 2016. **8**(4): p. 409-427.

7. Israelachvili, J.N., *Intermolecular and surface forces*. 2011: Academic press.

8. Hunter, R.J., L.R. White, and D.Y. Chan, *Foundations of colloid science.* (No Title), 1987.

9. Evans, D.F. and H. Wennerström, *The colloidal domain: where physics, chemistry, biology, and technology meet.* 1999.

10. Atkins, P.W., et al., *Physical chemistry for the life sciences*. 2023: Oxford University Press.

11. Kim, A., et al., *Validation of Size Estimation of Nanoparticle Tracking Analysis on Polydisperse Macromolecule Assembly.* Scientific Reports, 2019. **9**(1): p. 2639.

12. Kim, H.Y., *Statistical notes for clinical researchers: post-hoc multiple comparisons.* Restor Dent Endod, 2015. **40**(2): p. 172-6.

13. Šidák, Z., *Rectangular Confidence Regions for the Means of Multivariate Normal Distributions.* Journal of the American Statistical Association, 1967. **62**(318): p. 626-633.

14. Dunnett, C.W., *A multiple comparison procedure for comparing several treatments with a control.* Journal of the American Statistical Association, 1955. **50**(272): p. 1096-1121.